

Effect of the Breit interaction on the angular distribution of Auger electrons following electron-impact excitation of highly charged Be-like ions

Z. W. Wu ^{*}, Y. Li, Z. Q. Tian, and C. Z. Dong

Key Laboratory of Atomic and Molecular Physics and Functional Materials of Gansu Province, College of Physics and Electronic Engineering, Northwest Normal University, Lanzhou 730070, People's Republic of China

 (Received 15 December 2021; accepted 2 March 2022; published 15 March 2022)

The electron-impact excitation from the ground state to the autoionizing level $1s2s^22p_{1/2}J=1$ and the subsequent nonradiative Auger decay $1s2s^22p_{1/2}J=1 \rightarrow 1s^22sJ=1/2$ of Be-like ions have been studied by using the multiconfigurational Dirac-Fock method and the relativistic distorted-wave theory. Special attention has been paid to the effect of the Breit interaction on the angular distribution of the Auger electrons emitted. To do so, the partial cross sections, alignment parameters of the autoionizing level, and intrinsic anisotropy parameters of the Auger decay are evaluated for Be-like Mg^{8+} , Fe^{22+} , Mo^{38+} , Nd^{56+} , Au^{75+} , and U^{88+} ions, from which the angular distribution of the Auger electrons is further obtained. It is found that the Breit interaction hardly contributes to the angular distribution for low- Z ions such as Mg^{8+} , especially at low impact energies, while for medium- and high- Z ions the situation becomes fairly different. To be specific, the Breit interaction contributes to lowering the anisotropy of the angular distribution, which first becomes quickly more prominent with increasing atomic number up to certain high- Z ions and then behaves very slowly less prominently for higher- Z ions. Moreover, for high- Z ions the effect of the Breit interaction on the angular distribution is found to be nearly independent of the atomic number Z . Owing to opposite effects of the Breit interaction on the alignment parameters and the intrinsic anisotropy parameters, such an “abnormal behavior” is speculated to be caused very likely by a “competition” between the opposite effects of the Breit interaction on both of them.

DOI: [10.1103/PhysRevA.105.032809](https://doi.org/10.1103/PhysRevA.105.032809)

I. INTRODUCTION

Electron-impact excitation (EIE) of atoms or ions is one of fundamental atomic processes in astrophysical and laboratory plasmas. When one of the inner-shell electrons of atoms or ions is excited by electron impact, the resulting ions will reside in some excited hole states. These excited states are unstable and hence will decay to some energetically lower states with emission of photons or electrons. In particular, excited states of atoms or ions created by a beam of particles or photons are usually aligned along the direction of the beam if total angular momentum of the states is greater than $1/2$ [1,2]. Auger electrons or (x-ray) photons emitted from these aligned atoms or ions are thus expected to be spin polarized and anisotropic [1–3]. Spin polarization and angular distribution of Auger electrons can provide fundamental information on the excitation and subsequent nonradiative decay of atoms or ions. Such information is additional and much more detailed than information such as decay rates and Auger energies and, indeed, deserves to be revealed in detail [4,5].

During the past half century, angular distribution of Auger electrons emitted from atoms, molecules, and ions excited by colliding with (quasi-)free electrons or interacting with photons has been being extensively investigated both theoretically and experimentally [6–17]. For the first time, an experimental evidence for anisotropic angular distribution of $L_3M_{2,3}M_{2,3} (^1S_0)$ Auger electrons following an L_3 vacancy

in argon caused by electron impact was presented by Cleff and Mehlhorn in 1971 [18]. Flügge *et al.* analyzed angular distribution of Auger electrons following photoionization of magnesium and calcium and then proposed that relative partial photoionization cross sections could be determined directly from the obtained anisotropic angular distribution [3]. Later, more general theories and expressions were presented for the studies of angular distribution (and spin polarization) of Auger electrons [19–22]. In addition, Bhalla obtained an anisotropic angular distribution of Auger electrons in resonant transfer and excitation in collisions of ions with light targets [23]. Viehhaus *et al.* measured angular distribution of Auger electrons emitted in direct $L_{2,3}MMM$ double Auger decay after photoionization of a $2p$ electron of argon [24]. Based on the results obtained, they claimed that information on both the electron correlations giving rise to the double Auger process and the symmetry of the associated two-electron continuum state can be revealed [24]. Furthermore, Cryan *et al.* studied experimentally angular distribution of Auger electrons of double core-hole states of molecular nitrogen in the molecular reference frame by using the Linac Coherent Light Source free electron laser, which exhibits an entirely new way to study femtosecond chemical dynamics with Auger electrons that probe the local valence structure of molecules near a specific atomic core [25]. Just recently, the effect of angular momentum transfer on angular distribution of Auger electrons after inner-shell ns^2 photoionization of noble gases was studied and a noticeable influence was obtained [26].

In particular, Chen and Reed studied theoretically the relativistic effects on angular distribution of Auger electrons

*zhongwen.wu@nwnu.edu.cn

emitted from Be-like Mg^{8+} , Fe^{22+} , and Mo^{38+} ions following the $1s \rightarrow 2p$ excitation by electron impact [27]. It was found that the Auger electrons emitted are strongly anisotropic for most of the transitions considered and, especially, that the relativistic effects can fully change the characteristics of the angular distribution for the transitions with many contributing partial waves, even for ions as light as Fe^{22+} [27]. Nevertheless, as one of the dominant relativistic effects, the Breit interaction was not considered in this work. As is well known, the Breit interaction plays a very important role in fundamental atomic processes of highly charged high- Z ions with free electrons involved, such as EIE [28–32], electron-impact ionization [33–35], dielectronic recombination [36–45], and photoionization [46,47], which was first introduced by Breit in 1929 to characterize high-order correction to electron-electron interactions beyond the well-known Coulomb interaction [48,49]. Up to the present, however, the effect of the Breit interaction on angular distribution of Auger electrons following EIE of Be-like ions was never studied.

In the present paper, we follow the work of Chen and Reed [27] and study the angular distribution of Auger electrons following the EIE $1s^2 2s^2 J=0 \rightarrow 1s 2s^2 2p_{1/2} J=1$ of Be-like Mg^{8+} , Fe^{22+} , Mo^{38+} , Nd^{56+} , Au^{75+} , and U^{88+} ions by using the multiconfigurational Dirac-Fock (MCDF) method and the relativistic distorted-wave (RDW) theory. In particular, special attention is paid to the effect of the Breit interaction on the angular distribution. To do so, we first calculate partial EIE cross sections for the excitations from the ground state to magnetic substates $|M_f = \pm 1, 0\rangle$ of the autoionizing level $1s 2s^2 2p_{1/2} J=1$. By employing these partial EIE cross sections, alignment parameters of the autoionizing level are further obtained. Furthermore, we evaluate intrinsic anisotropy parameters of the Auger decay $1s 2s^2 2p_{1/2} J=1 \rightarrow 1s^2 2s J=1/2$. Moreover, the angular distributions of the Auger electrons are finally obtained by means of these alignment parameters and intrinsic anisotropy parameters. It is found that for low- Z ions such as Mg^{8+} the Breit interaction hardly contributes to the angular distribution of the Auger electrons, while for medium- and high- Z Be-like ions its contribution is indispensable. To be specific, at given impact electron energies the Breit interaction makes the angular distribution less anisotropic, which becomes first more prominent with increasing atomic number and, then, less and less as it increases further.

The present paper is structured as follows. In the next section, the theoretical method is presented especially for studying the angular distribution of Auger electrons following the EIE of Be-like ions. In Sec. III, we discuss the presently obtained results for the EIE cross sections, the alignment parameters, the intrinsic anisotropy parameters, and the angular distribution and, in particular, reveal the effect of the Breit interaction on them. Atomic units ($m_e = 1$, $e = 1$, $\hbar = 1$) have been used throughout the present paper unless specified otherwise.

II. THEORETICAL METHOD

Let us start with the following two-step EIE and Auger decay process of Be-like

ions:

$$e + 1s^2 2s^2 J=0 \longrightarrow 1s 2s^2 2p_{1/2} J=1 + e_{sc} \\ \longrightarrow 1s^2 2s J=1/2 + e_{sc} + e_A. \quad (1)$$

In the first step, Be-like ions are excited by electron impact from their ground state $1s^2 2s^2 J=0$ to the autoionizing level $1s 2s^2 2p_{1/2} J=1$. The subsequent nonradiative decay in the second step from the autoionizing level to the ground state $1s^2 2s J=1/2$ of the corresponding Li-like ions gives rise to the emission of Auger electrons. To explore the effect of the Breit interaction on the angular distribution of the emitted Auger electrons, we treat the excitation and decay of ions independently.

To describe the process (1), the atomic structure package GRASP92 [50] is used to generate all the bound-state energy levels and wave functions required, which was developed based on the MCDF method. Since this method has been described in detail in many places (see, e.g., Refs. [51,52]), we shall not show it here for brevity. For the first step of the process (1), i.e., the EIE of Be-like ions, a fully RDW program REIE06 [53,54] is utilized to calculate partial EIE cross sections. In the RDW theory, if the direction of incident (impact) electrons is chosen to be the quantization z axis, the projection m_i (m'_i) of orbital angular momentum l_i (l'_i) of the incident electrons onto the z axis is zero, i.e., $m_i = m'_i = 0$. In this case, the partial EIE cross sections from a well-defined initial state $|\beta_i J_i M_i\rangle$ to a final state $|\beta_f J_f M_f\rangle$ of target ions can be expressed as [54,55]

$$\sigma_{|i\rangle \rightarrow |f\rangle} = \frac{2\pi a_0^2}{k_i^2} \sum_{l_i j_i l'_i j'_i m_s l_f j_f m_j} \sum_{J J M} \\ \times i^{l_i - l'_i} [l_i, l'_i]^{1/2} \exp[i(\delta_{l_i j_i} - \delta_{l'_i j'_i})] \\ \times \langle l_i m_i, 1/2 m_s | j_i m_j \rangle \langle l'_i m'_i, 1/2 m_s | j'_i m'_j \rangle \\ \times \langle J_i M_i, j_i m_j | J M \rangle \langle J_i M_i, j'_i m'_j | J' M \rangle \\ \times \langle J_f M_f, j_f m_j | J M \rangle \langle J_f M_f, j_f m_j | J' M \rangle \\ \times R(\gamma_i, \gamma_f) R^*(\gamma'_i, \gamma'_f). \quad (2)$$

In this expression, the subscripts i and f indicate the initial and final ($1s 2s^2 2p_{1/2} J=1 + e_{sc}$) states of the impact system (i.e., target ion plus electron), respectively. We denote by $1/2$, l_i (l'_i), and j_i (j'_i) the spin, orbital, and total angular momenta of the incident impact electrons, respectively, while m_s , m_i (m'_i), and m_j (m'_j) are their respective z projections. J_i and M_i are the total angular momentum of the initial state $|\beta_i J_i M_i\rangle$ of the target ions and its projection onto the z axis, respectively, while β_i denotes all other quantum numbers required for a unique specification of this state. Likewise, J (J') and M are the total angular momentum of the impact system and its projection, $\gamma_i \equiv \varepsilon_i l_i j_i \beta_i J_i J M$ and $\gamma_f \equiv \varepsilon_f l_f j_f \beta_f J_f J M$. Furthermore, other quantum numbers with the subscript f have similar meanings to those as stated above but for the final states of the systems involved. Moreover, k_i denotes the relativistic wave number of the impact electron and is related to its kinetic energy ε_i via $k_i^2 = \varepsilon_i(1 + \alpha^2 \varepsilon_i/4)$ with the fine-structure constant α . $\delta_{l_i j_i}$ ($\delta_{l'_i j'_i}$) is the phase shift of the impact electrons. a_0 denotes the Bohr radius. It is noted

that the standard notation of the Clebsch-Gordan coefficients and the shorthand notation $[a, b, \dots] \equiv (2a+1)(2b+1)\dots$ have been used. Owing to the property of the Clebsch-Gordan coefficients, $m_{j_i} (m'_{j_i}) \equiv m_{s_i}$ and, thus, the summations over $m_{j_i} (m'_{j_i})$ are not shown explicitly. In addition, $R(\gamma_i, \gamma_f)$ denotes the EIE amplitudes, formally expressed as follows:

$$R(\gamma_i, \gamma_f) = \langle \psi_{\gamma_f} | \sum_{p,q;p < q}^{N+1} \left(\frac{1}{r_{pq}} + V_{\text{Breit}} \right) | \psi_{\gamma_i} \rangle. \quad (3)$$

Here, ψ_{γ_i} and ψ_{γ_f} denote the wave functions of the initial and final states of the impact system, respectively. $1/r_{pq}$ is the Coulomb operator, while the Breit interaction operator V_{Breit} is given by

$$V_{\text{Breit}} = \frac{\boldsymbol{\alpha}_p \cdot \boldsymbol{\alpha}_q}{r_{pq}} \cos(\omega_{pq} r_{pq}) + (\boldsymbol{\alpha}_p \cdot \nabla_p)(\boldsymbol{\alpha}_q \cdot \nabla_q) \frac{\cos(\omega_{pq} r_{pq}) - 1}{\omega_{pq}^2 r_{pq}}, \quad (4)$$

where $\boldsymbol{\alpha}_p$ and $\boldsymbol{\alpha}_q$ are the Dirac matrices, and ω_{pq} denotes the angular frequency of the virtual photons exchanged.

Having the partial EIE cross sections ready, as given by Eq. (2), the relative population of the magnetic substates $|\beta_f J_f M_f\rangle$ of the excited energy level $\beta_f J_f$ can be readily obtained, which will partially determine the angular distribution of the subsequently emitted Auger electrons. Within the density-matrix theory [56], such a population is characterized most generally by a set of alignment parameters. For the presently considered autoionizing level $1s^2s^2p_{1/2} J=1$, there is only one, that is, a second-rank alignment parameter \mathcal{A}_{20} , which is given by [37]

$$\mathcal{A}_{20} = \sqrt{2} \frac{\sigma_{\pm 1} - \sigma_0}{2\sigma_{\pm 1} + \sigma_0}. \quad (5)$$

Here, σ_0 and $\sigma_{\pm 1}$ represent the partial EIE cross sections for the excitations from the ground state to the magnetic substates $|M_f=0\rangle$ and $|M_f=\pm 1\rangle$ of the autoionizing level $1s^2s^2p_{1/2} J=1$, respectively. The second-rank parameter \mathcal{A}_{20} fully describes the relative population of the magnetic substates of the $1s^2s^2p_{1/2} J=1$ level. It should be noted that integrations over angular and polarization variables of the scattered electron (e_{sc}) are carried out in obtaining the alignment parameter \mathcal{A}_{20} since it is assumed to be unobserved.

For randomly oriented Be-like ions and unpolarized impact electrons, if the detectors employed are not sensitive to spin polarization of electrons, the angular distribution of the Auger electrons emitted in the second step of the process (1) can be written as [57,58]

$$W(\theta) \propto 1 + \alpha_2 \mathcal{A}_{20} P_2(\cos \theta). \quad (6)$$

Here, $P_2(\cos \theta)$ is the second-order Legendre polynomial as a function of the angle θ between the emitted Auger electrons and the incident impact electrons. α_2 denotes the intrinsic anisotropy parameter of the nonradiative Auger decay and is

determined by [59]

$$\begin{aligned} \alpha_2 = & (-1)^{J+J_f-1/2} [J]^{1/2} \sum_{l'l'jj'} [l, l', j, j']^{1/2} \langle l0, l'0 | 20 \rangle \\ & \times \left\{ \begin{matrix} J & j & J_f \\ j' & J & 2 \end{matrix} \right\} \left\{ \begin{matrix} l & j & 1/2 \\ j' & l' & 2 \end{matrix} \right\} \\ & \times \langle \alpha_f J_f, l j : J \| V \| \alpha J \rangle \langle \alpha_f J_f, l' j' : J \| V \| \alpha J \rangle^* \\ & \times \sum_{lj} |\langle \alpha_f J_f, l j : J \| V \| \alpha J \rangle|^{-2}. \end{aligned} \quad (7)$$

In this expression, J and J_f are total angular momenta of the initial and final levels αJ and $\alpha_f J_f$ of the Auger decay, respectively. l (l') and j (j') are orbital and total angular momenta of the emitted Auger electrons, respectively. Moreover, standard notations have been used for the Clebsch-Gordan coefficients and the Wigner-6j symbols. The reduced matrix elements $\langle \alpha_f J_f, l j : J \| V \| \alpha J \rangle$ denote Auger decay amplitudes, which are evaluated by utilizing the RATIP package [60]. Note that the electron-electron interaction operator V consists of the Coulomb and Breit operators.

In the present theoretical calculations, configurations $1s^22s^2$, $1s^22p^2$, $1s^22s2p$, and $1s2s^22p$ are used to generate wave functions and energy levels required for the EIE of Be-like ions, while $1s^22s$, $1s^23s$, and $1s^23d$ are utilized for the final state $1s^22s J=1/2$ of the Auger decay. In these calculations, the quantum-electrodynamical effects are incorporated. Moreover, in the calculations of partial EIE cross sections, maximal partial waves are taken to be $\kappa = \pm 50$ to ensure convergence. It should be noted that all the calculations are carried out twice, that is, without (labelled by NB) and with (by B) the Breit interaction included in both the EIE and Auger decay amplitudes, respectively.

III. RESULTS AND DISCUSSION

In Table I, we tabulate the presently calculated excitation energies from the ground state $1s^22s^2 J=0$ to the autoionizing level $1s2s^22p_{1/2} J=1$ of Be-like Mg^{8+} , Fe^{22+} , Mo^{38+} , Nd^{56+} , Au^{75+} , and U^{88+} ions and Auger electron energies from the autoionizing level to the ground state $1s^22s J=1/2$ of the corresponding Li-like ions, together with other results from Refs. [61–64] for comparison. Results are shown for two cases, i.e., without (NB) and with (B) an inclusion of the contribution from the Breit interaction. As seen clearly from the table, the present excitation energies agree very well with these results; the maximum discrepancy is found to be less than 0.32% among the Be-like ions considered. Moreover, it is found that both the excitation energies and Auger electron energies without the Breit interaction included are overestimated, which becomes more prominent with increasing atomic number. To be specific, the relative contribution of the Breit interaction to the excitation energy changes from 0.04% for low- Z Mg^{8+} ions to 0.37% for high- Z U^{88+} ions, while its contribution to the Auger electron energy changes from 0.05 to 0.49% along the same Be-like ions considered.

Figure 1 displays the presently calculated partial and total EIE cross sections for the excitations from the ground state $1s^22s^2 J=0$ to the individual substates $|M_f=0\rangle$ and $|M_f=\pm 1\rangle$ of the autoionizing level $1s2s^22p_{1/2} J=1$ of

TABLE I. Presently calculated excitation energies from the ground state $1s^2 2s^2 J=0$ to the autoionizing level $1s2s^2 2p_{1/2} J=1$ of Be-like Mg^{8+} , Fe^{22+} , Mo^{38+} , Nd^{56+} , Au^{75+} , and U^{88+} ions and Auger energies from the autoionizing level to the ground state $1s^2 2s J=1/2$ of the corresponding Li-like ions, compared with the results from Refs. [61–64]. Results are given for two cases, i.e., without (NB) and with (B) an inclusion of the contribution from the Breit interaction.

Ions	Excitation energies (eV)				Auger energies (eV)	
	NB	NB	B	B	NB	B
Mg^{8+}	1317.81		1317.24	1321.36 [61]	990.80	990.29
Fe^{22+}	6614.08	6635.06 [62]	6607.82	6628.83 [62]	4662.83	4657.26
Mo^{38+}	17842.66	17842.4 [63]	17814.22	17813.9 [63]	12288.12	12262.80
Nd^{56+}	37685.76	37674 [64]	37598.03	37587 [64]	25575.54	25497.73
Au^{75+}	68354.22		68140.59		45790.81	45602.38
U^{88+}	96523.25	96522.7 [63]	96165.99	96165.2 [63]	64034.16	63720.66

Be-like Mg^{8+} , Fe^{22+} , Mo^{38+} , Nd^{56+} , Au^{75+} , and U^{88+} ions, as functions of impact electron energy in units of their respective excitation thresholds. Results are shown for both the NB

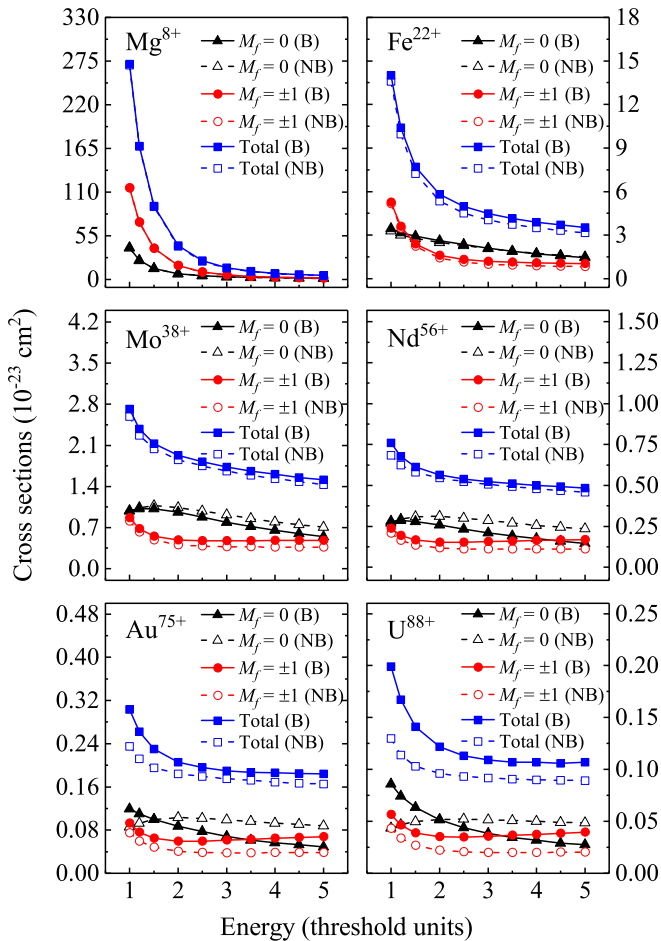


FIG. 1. Partial and total EIE cross sections for the excitations from the ground state $1s^2 2s^2 J=0$ to the individual magnetic substates $|M_f=0\rangle$ and $|M_f=\pm 1\rangle$ of the autoionizing level $1s2s^2 2p_{1/2} J=1$ of Be-like Mg^{8+} (top left panel), Fe^{22+} (top right), Mo^{38+} (middle left), Nd^{56+} (middle right), Au^{75+} (bottom left), and U^{88+} ions (bottom right), as functions of impact electron energy in units of their respective excitation thresholds as listed in Table I. Results are given for both the NB (dashed lines with hollow symbols) and B (solid lines with solid symbols) cases for comparison.

(dashed lines with hollow symbols) and B (solid lines with solid symbols) cases for comparison. Note that the partial EIE cross sections corresponding to the substate $|M_f=-1\rangle$ are fully identical to the ones corresponding to the substate $|M_f=+1\rangle$ owing to spatial symmetry of the EIE process considered. It is found that for low- Z Be-like ions such as Mg^{8+} the Breit interaction makes almost no contribution to both the partial and total EIE cross sections at all the impact energies considered. For medium- and high- Z ions, however, the Breit interaction contributes to increasing the total EIE cross sections at all the impact energies, which becomes more prominent with increasing atomic number. As for their corresponding partial EIE cross sections, moreover, the situation becomes quite different. To be specific, the Breit interaction makes the partial EIE cross sections corresponding to the individual substate $|M_f=\pm 1\rangle$ increase at all the impact energies considered, which behaves more and more pronounced with increasing impact energy and atomic number, respectively. In contrast, for medium- Z ions it contributes to decreasing the partial cross sections corresponding to the substate $|M_f=0\rangle$ at all the impact electron energies, while for high- Z ions the partial ones first increase at low impact energies and then decrease at medium and high energies due to the contribution of the Breit interaction, as can be seen clearly from the results of Au^{75+} and U^{88+} ions. Admittedly, such a quite different effect of the Breit interaction on the partial EIE cross sections will remarkably alter the relative population of the substates $|M_f=0\rangle$ and $|M_f=\pm 1\rangle$ of the autoionizing level $1s2s^2 2p_{1/2} J=1$ when compared to the case without the Breit interaction included.

Having the partial EIE cross sections available, the corresponding second-rank alignment parameters \mathcal{A}_{20} of the autoionizing level $1s2s^2 2p_{1/2} J=1$ can be easily obtained. To explain reliability of the present calculations, we first compare the present alignment parameters with other results [27] available for Mg^{8+} , Fe^{22+} , and Mo^{38+} ions in the case without the Breit interaction included, as listed in Table II. The impact electron energies used for these three ions are 5, 9, and 20 keV, respectively. It is found that for medium- Z Mo^{38+} ions the present alignment parameter -0.203 with the use of the maximal partial waves $\kappa = \pm 50$ coincides excellently with the result -0.199 from Ref. [27], while for low- Z Mg^{8+} and Fe^{22+} ions both the two results differ remarkably from each other. Since the full computational details were not presented in Ref. [27], in order to find out possible reasons for such

TABLE II. Comparison of the present alignment parameters \mathcal{A}_{20} of the autoionizing level $1s2s^22p_{1/2}J=1$ with other results [27] available for Be-like Mg^{8+} , Fe^{22+} , and Mo^{38+} ions in the case without the Breit interaction included. The present results are presented for three different maximal partial waves, i.e., $\kappa = \pm 5$, ± 10 , and ± 50 . The impact electron energies used for these ions are 5, 9, and 20 keV, respectively.

Ions	Ref. [27]	$\kappa = \pm 5$	$\kappa = \pm 10$	$\kappa = \pm 50$
Mg^{8+}	0.255	0.248	0.133	0.121
Fe^{22+}	-0.062	-0.014	-0.028	-0.028
Mo^{38+}	-0.199	-0.200	-0.203	-0.203

remarkable differences we performed additional calculations by using a series of different maximal partial waves. It is shown that for low- Z Mg^{8+} ions the present alignment parameter 0.248 with the use of $\kappa = \pm 5$ is most consistent with the result 0.255 in Ref. [27], which indicates that for low- Z ions such as Mg^{8+} the use of a small number of partial waves could give rise to nonconvergent results and thus more higher partial waves are required to ensure convergence. For Fe^{22+} ions, however, the alignment parameter is -0.014 for the maximal partial waves $\kappa = \pm 5$ and then converges rapidly to -0.028 at $\kappa = \pm 10$ according to the present calculations, neither of which agrees with the result -0.062 in Ref. [27]. Such a difference is still an open question and, hence, more additional work is required to address it properly.

In Fig. 2, we plot the presently obtained alignment parameters \mathcal{A}_{20} of the autoionizing level $1s2s^22p_{1/2}J=1$ following the EIE of Be-like Mg^{8+} , Fe^{22+} , Mo^{38+} , Nd^{56+} , Au^{75+} , and U^{88+} ions, as functions of the impact electron energy in the threshold units. Results are given for both the NB and B cases for comparison. Note that the coordinate scales used for Mg^{8+} and Fe^{22+} ions are different from those for the other four ions. As seen clearly from the figure, the Breit interaction hardly contributes to the alignment parameters for low- Z ions such as Mg^{8+} even at high impact electron energies, while the contribution of the Breit interaction is essential for medium- and high- Z ions and, in particular, behaves more prominently for higher- Z ions and also at higher impact energies, respectively. For instance, the absolute contribution of the Breit interaction to the alignment parameter \mathcal{A}_{20} changes from 0.133 for Fe^{22+} ions to 0.603 for U^{88+} ions at the impact electron energy of 5.0 times their respective excitation thresholds, i.e., a remarkable increase by a factor of 3.5. Furthermore, taking high- Z Au^{75+} ions, for example, such an absolute contribution increases significantly from 0.043 to 0.568 with increasing impact energy from 1.2 to 5.0 times the excitation threshold. In addition, it should be mentioned that for medium- and high- Z ions such as Nd^{56+} , Au^{75+} , and U^{88+} the sign of the alignment parameters is altered to be positive from being negative at high impact energies due to the remarkable contribution of the Breit interaction. Such a change of the sign indicates that the magnetic substates $|M_f = \pm 1\rangle$ are predominantly populated over the one $|M_f = 0\rangle$ in high-energy EIE of medium- and high- Z Be-like ions, as can be seen explicitly from Fig. 1.

In order to obtain the angular distribution of the emitted Auger electrons following the EIE of Be-like ions, besides

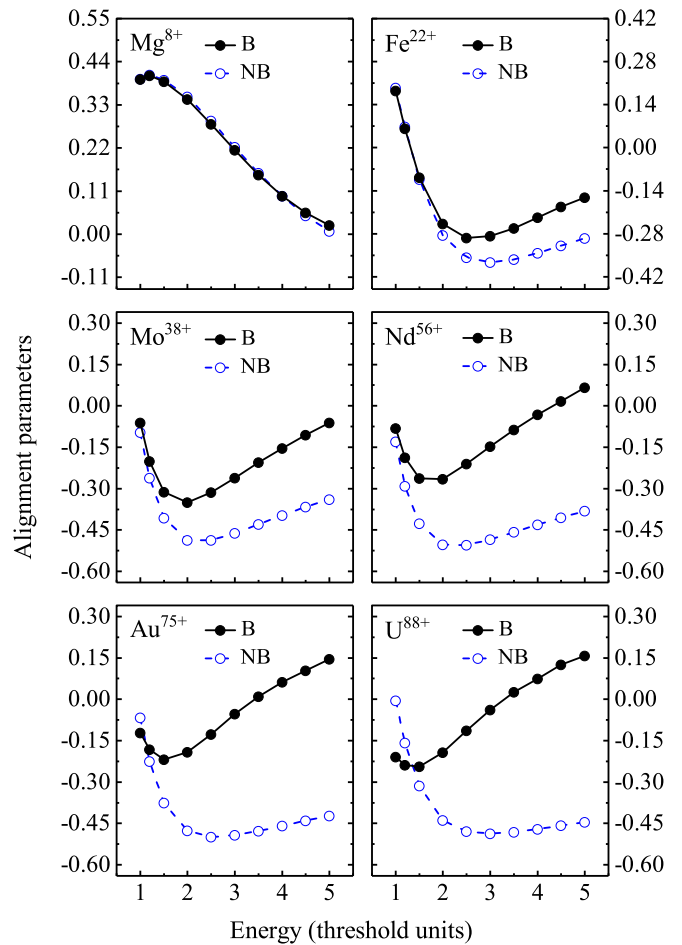


FIG. 2. Alignment parameters \mathcal{A}_{20} of the autoionizing level $1s2s^22p_{1/2}J=1$ following the EIE of Mg^{8+} , Fe^{22+} , Mo^{38+} , Nd^{56+} , Au^{75+} , and U^{88+} ions, as functions of the impact electron energy in the threshold units. Results are given for both the NB (blue dashed lines with hollow circles) and B (black solid lines with solid circles) cases. Please see Supplemental Material for the data used to plot this and the following figures [65].

the alignment parameters \mathcal{A}_{20} of the autoionizing level, the intrinsic anisotropy parameters α_2 of the corresponding Auger decay are required as well, as can be seen from Eq. (6). In Fig. 3, we display the presently calculated intrinsic anisotropy parameters of the nonradiative Auger decay [i.e., the second step in Eq. (1)] of the six Be-like ions, as functions of the atomic number Z . Again, the present results are given for both the NB and B cases together with other results [27] available for Mg^{8+} , Fe^{22+} , and Mo^{38+} ions in the NB case for comparison. As seen obviously from the figure, the present intrinsic anisotropy parameters for the NB case without the Breit interaction included agree excellently with the available results from Ref. [27]; the relative discrepancy is 1.65% for Fe^{22+} and less than 0.2% for the other two ions. Similar to the effect of the Breit interaction on the alignment parameters, it is found that the Breit interaction hardly contributes to the intrinsic anisotropy parameters for low- Z ions such as Mg^{8+} and Fe^{22+} , while for medium- and high- Z ions its contribution is indispensable. To be specific, the Breit interaction makes the intrinsic anisotropy parameters decrease

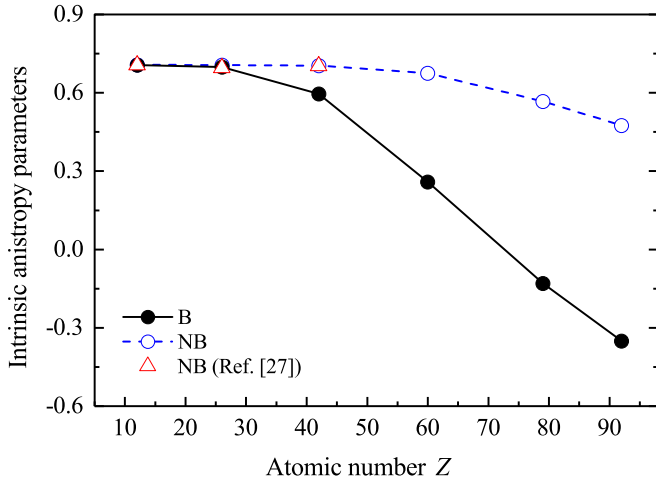


FIG. 3. Intrinsic anisotropy parameters α_2 of the nonradiative Auger decay of Be-like Mg^{8+} , Fe^{22+} , Mo^{38+} , Nd^{56+} , Au^{75+} , and U^{88+} ions. The present results are given for both the NB (blue hollow circles) and B (black solid circles) cases together with other results [27] (red hollow triangles) available for the first three Be-like ions in the NB case for comparison. Lines are drawn as a guide to the eyes.

significantly, which behaves more prominently with increasing atomic number and, in particular, even alters the sign of the intrinsic anisotropy parameters for high- Z ions. Moreover, the intrinsic anisotropy parameter without the Breit interaction included is found to be weakly dependent on the atomic number Z , which decreases very slowly from 0.707 for Mg^{8+} ions to 0.475 for U^{88+} ions. In contrast, a very strong Z dependence is found for the intrinsic anisotropy parameter with the Breit interaction included, which decreases quickly from 0.707 to -0.351 for the same Be-like ions. Such a remarkable effect of the Breit interaction is expected to influence significantly the angular distribution of the Auger electrons emitted from medium- and high- Z ions, together with its effect on the alignment parameters stated above.

Once the alignment parameters \mathcal{A}_{20} and the intrinsic anisotropy parameters α_2 are available, the angular distribution of the Auger electrons emitted from Be-like ions can be readily obtained by using Eq. (6). As an example, Fig. 4 displays the presently obtained angular distribution of the Auger electrons emitted from the Auger decay $1s2s^22p_{1/2}J=1 \rightarrow 1s^22sJ=1/2$ following the EIE of Be-like Mg^{8+} , Fe^{22+} , Mo^{38+} , Nd^{56+} , Au^{75+} , and U^{88+} ions for the impact electron energy of 3.0 times their respective excitation thresholds. Once again, results are given for both the two cases without and with the Breit interaction included for comparison. As expected from the analysis on the effects of the Breit interaction upon both the alignment parameters \mathcal{A}_{20} and the intrinsic anisotropy parameters α_2 , the Breit interaction hardly contributes to the angular distribution of the Auger electrons for low- Z ions such as Mg^{8+} . For both the two cases, the Auger electrons are dominantly emitted along the incident electron-beam axis z , that is to say, under $\theta=0^\circ$ and 180° . As for medium- and high- Z Be-like ions, however, the situation becomes fairly different. Specifically, in the case without the Breit interaction considered the Auger electrons are dominantly emitted perpendicular to the electron beam axis, i.e.,

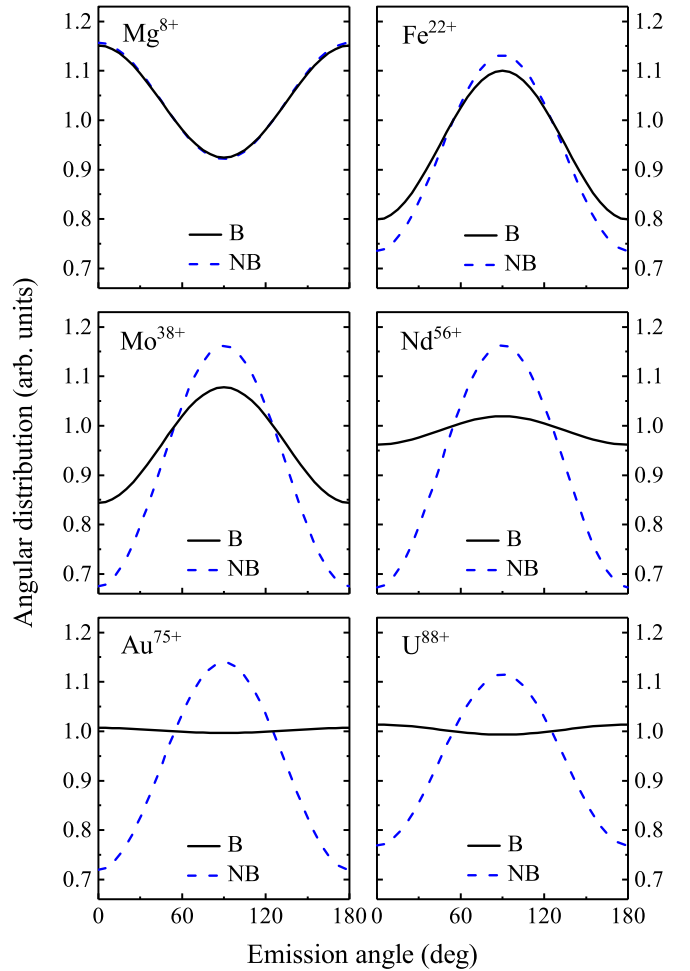


FIG. 4. Angular distribution $W(\theta)$ of the Auger electrons emitted from the Auger decay $1s2s^22p_{1/2}J=1 \rightarrow 1s^22sJ=1/2$ following the EIE of Be-like Mg^{8+} , Fe^{22+} , Mo^{38+} , Nd^{56+} , Au^{75+} , and U^{88+} ions for the impact electron energy of 3.0 times their respective excitation thresholds. Results are presented for both the NB (blue dashed lines) and B (black solid lines) cases.

under $\theta=90^\circ$, and the corresponding angular distribution of the Auger electrons is found to be nearly independent of the atomic number. Moreover, it is found that the Breit interaction contributes to weakening the anisotropy of the angular distribution, which first becomes quickly more prominent with increasing atomic number up to certain high- Z ions and, then, behaves very slowly less prominently for higher- Z ions.

In particular, here it is worth mentioning that a nearly isotropic angular distribution is predicted for Be-like ions with atomic numbers around 70 due to the contribution of the Breit interaction, which remains the same also for higher- Z ions up to U^{88+} , as seen obviously from the results of Au^{75+} and U^{88+} ions in Fig. 4. Such a consistent isotropic angular distribution shows that the effect of the Breit interaction on the angular distribution of the Auger electrons emitted from high- Z ions is almost independent of the atomic number Z , which is quite different from the situation for the angular distribution of the characteristic x-ray photons radiated from the identical autoionizing level $1s2s^22p_{1/2}J=1$ following the identical EIE process of Be-like ions [63]. For the latter, a

strong Z dependence was obtained for high- Z Be-like ions. By comparison, the Breit interaction affects the angular distribution of the x-ray photons only via the alignment parameter \mathcal{A}_{20} , while its influence on the one of the Auger electrons takes place via both the alignment parameter \mathcal{A}_{20} and the intrinsic anisotropy parameter α_2 . For this reason, the presently obtained Z independence for the effect of the Breit interaction on the angular distribution of the Auger electrons from high- Z ions is speculated to be resulted very likely from a “competition” between the effects of the Breit interaction on \mathcal{A}_{20} and α_2 . To prove this speculation, a systematic theoretical study is currently under way.

IV. SUMMARY

In summary, motivated by the work of Chen and Reed [27], the EIE from the ground state $1s^2 2s^2 J=0$ to the autoionizing level $1s 2s^2 2p_{1/2} J=1$ and the subsequent non-radiative Auger decay $1s 2s^2 2p_{1/2} J=1 \rightarrow 1s^2 2s J=1/2$ of Be-like Mg^{8+} , Fe^{22+} , Mo^{38+} , Nd^{56+} , Au^{75+} , and U^{88+} ions have been studied by using the MCDF method and the RDW theory. Special attention has been paid to the effect of the Breit interaction on the angular distribution of the emitted Auger electrons. To do this, we first calculated the partial EIE cross sections for the excitations from the ground state to the magnetic substates $|M_f=0\rangle$ and $|M_f=\pm 1\rangle$ of the autoionizing level $1s 2s^2 2p_{1/2} J=1$ of these Be-like ions, from which the alignment parameters of the autoionizing level were further obtained. Additionally, we evaluated the intrinsic anisotropy parameters of the Auger decay. By using the

alignment parameters and the intrinsic anisotropy parameters, the angular distribution of the emitted Auger electrons was finally obtained. It is found that for low- Z ions such as Mg^{8+} the Breit interaction hardly contributes to the angular distribution, especially for low impact energies, while for medium- and high- Z ions the situation becomes fairly different. Taking the impact energy of 3.0 times the excitation thresholds, for example, the Breit interaction contributes to weakening the anisotropy of the angular distribution, which first becomes quickly more prominent with increasing atomic number up to certain high- Z ions and then behaves very slowly less prominently for higher- Z ions. In addition, for high- Z ions with atomic numbers greater than around 70 the effect of the Breit interaction on the angular distribution is found to be nearly independent of the atomic number. Due to the opposite effects of the Breit interaction on the alignment parameters and the intrinsic anisotropy parameters, this “abnormal behavior” is speculated to be caused very likely by a competition between the opposite effects of the Breit interaction on both of them.

ACKNOWLEDGMENTS

This work has been funded by the National Natural Science Foundation of China under Grants No. 12174315 and No. 11804280, the Longyuan Youth Innovation and Entrepreneurship Talent Project of Gansu Province, the Youth Science and Technology Talent Promotion Project of Gansu Province under Grant No. GXH2020626-09, and the Key Program of the Research Ability Promotion Project for Young Scholars of Northwest Normal University of China under Grant No. NWNLU-LKQN2019-5.

-
- [1] W. Mehlhorn, *Phys. Lett. A* **26**, 166 (1968).
 [2] T. Kämpfer, I. Uschmann, Z. W. Wu, A. Surzhykov, S. Fritzsche, E. Förster, and G. G. Paulus, *Phys. Rev. A* **93**, 033409 (2016).
 [3] S. Flügge, W. Mehlhorn, and V. Schmidt, *Phys. Rev. Lett.* **29**, 7 (1972).
 [4] N. M. Kabachnik and I. P. Sazhina, *J. Phys. B* **21**, 267 (1988).
 [5] J. Tulkki, N. M. Kabachnik, and H. Aksela, *Phys. Rev. A* **48**, 1277 (1993).
 [6] P. Bolognesi, P. O’Keeffe, and L. Avaldi, *J. Phys. Chem. A* **113**, 15136 (2009).
 [7] S. Heinämäki, K. Jänkälä, and J. Niskanen, *J. Phys. B* **42**, 085002 (2009).
 [8] A. Y. Elizarov and I. I. Tupitsyn, *J. Exp. Theor. Phys.* **99**, 1119 (2004).
 [9] R. Sankari, A. Kivimäki, M. Huttula, H. Aksela, S. Aksela, M. Coreno, G. Turri, R. Camilloni, M. de Simone, and K. C. Prince, *Phys. Rev. A* **63**, 032715 (2001).
 [10] S. Fritzsche, *Phys. Lett. A* **180**, 262 (1993).
 [11] M. H. Chen, *Phys. Rev. A* **45**, 1684 (1992).
 [12] K.-N. Huang, *Phys. Rev. A* **26**, 2274 (1982).
 [13] W. Mehlhorn and K. Taulbjerg, *J. Phys. B* **13**, 445 (1980).
 [14] R. Bruch and H. Klar, *J. Phys. B* **13**, 2885 (1980).
 [15] R. Bruch and H. Klar, *J. Phys. B* **13**, 1363 (1980).
 [16] B. Cleff and W. Mehlhorn, *J. Phys. B* **7**, 593 (1974).
 [17] B. Cleff and W. Mehlhorn, *J. Phys. B* **7**, 605 (1974).
 [18] B. Cleff and W. Mehlhorn, *Phys. Lett. A* **37**, 3 (1971).
 [19] N. M. Kabachnik and I. P. Sazhina, *J. Phys. B* **17**, 1335 (1984).
 [20] K. Blum, B. Lohmann, and E. Taute, *J. Phys. B* **19**, 3815 (1986).
 [21] B. Lohmann, *Can. J. Phys.* **74**, 962 (1996).
 [22] V. V. Balashov, A. N. Grum-Grzhimailo, and N. M. Kabachnik, *J. Phys. B* **30**, 1269 (1997).
 [23] C. P. Bhalla, *Phys. Rev. Lett.* **64**, 1103 (1990).
 [24] J. Viehhaus, S. Cvejanović, B. Langer, T. Lischke, G. Prümper, D. Rolles, A. V. Golovin, A. N. Grum-Grzhimailo, N. M. Kabachnik, and U. Becker, *Phys. Rev. Lett.* **92**, 083001 (2004).
 [25] J. P. Cryan, J. M. Glowina, J. Andreasson, A. Belkacem, N. Berrah, C. I. Blaga, C. Bostedt, J. Bozek, C. Buth, L. F. DiMauro, L. Fang, O. Gessner, M. Guehr, J. Hajdu, M. P. Hertlein, M. Hoener, O. Kornilov, J. P. Marangos, A. M. March, B. K. McFarland, H. Merdji, V. Petrovic, C. Raman, D. Ray, D. Reis, F. Tarantelli, M. Trigo, J. White, W. White, L. Young, P. H. Bucksbaum, and R. N. Coffee, *Phys. Rev. Lett.* **105**, 083004 (2010).
 [26] L. Gerchikov and S. Sheinerman, *Phys. Rev. A* **103**, 032807 (2021).
 [27] M. H. Chen and K. J. Reed, *Phys. Rev. A* **50**, 2279 (1994).
 [28] C. J. Fontes, H. L. Zhang, and D. H. Sampson, *Phys. Rev. A* **59**, 295 (1999).
 [29] C. J. Bostock, D. V. Fursa, and I. Bray, *Phys. Rev. A* **80**, 052708 (2009).

- [30] A. Gumberidze, D. B. Thorn, C. J. Fontes, B. Najjari, H. L. Zhang, A. Surzhykov, A. Voitkiv, S. Fritzsche, D. Banaś, H. Beyer, W. Chen, R. D. DuBois, S. Geyer, R. E. Grisenti, S. Hagmann, M. Hegewald, S. Hess, C. Kozhuharov, R. Martin, I. Orban, N. Petridis, R. Reuschl, A. Simon, U. Spillmann, M. Trassinelli, S. Trotsenko, G. Weber, D. F. A. Winters, N. Winters, D. Yu, and T. Stohlker, *Phys. Rev. Lett.* **110**, 213201 (2013).
- [31] C. Ren, Z. W. Wu, J. Jiang, L. Y. Xie, D. H. Zhang, and C. Z. Dong, *Phys. Rev. A* **98**, 012711 (2018).
- [32] A. Gumberidze, D. B. Thorn, A. Surzhykov, C. J. Fontes, B. Najjari, A. Voitkiv, S. Fritzsche, D. Banaś, H. F. Beyer, W. Chen, R. E. Grisenti, S. Hagmann, R. Hess, P. M. Hillenbrand, P. Indelicato, C. Kozhuharov, M. Lestinsky, R. Martin, N. Petridis, R. V. Popov, R. Schuch, U. Spillmann, S. Tashenov, S. Trotsenko, A. Warczak, G. Weber, W. Wen, D. F. A. Winters, N. Winters, Z. Yin, and T. Stohlker, *Phys. Rev. A* **99**, 032706 (2019).
- [33] C. J. Fontes, D. H. Sampson, and H. L. Zhang, *Phys. Rev. A* **59**, 1329 (1999).
- [34] M. K. Inal, H. L. Zhang, D. H. Sampson, and C. J. Fontes, *Phys. Rev. A* **65**, 032727 (2002).
- [35] O. Y. Andreev, E. A. Mistonova, and A. B. Voitkiv, *Phys. Rev. Lett.* **112**, 103202 (2014).
- [36] N. Nakamura, A. P. Kavanagh, H. Watanabe, H. A. Sakaue, Y. Li, D. Kato, F. J. Currell, and S. Ohtani, *Phys. Rev. Lett.* **100**, 073203 (2008).
- [37] S. Fritzsche, A. Surzhykov, and T. Stöhlker, *Phys. Rev. Lett.* **103**, 113001 (2009).
- [38] D. Bernhardt, C. Brandau, Z. Harman, C. Kozhuharov, A. Müller, W. Scheid, S. Schippers, E. W. Schmidt, D. Yu, A. N. Artemyev, I. I. Tupitsyn, S. Bohm, F. Bosch, F. J. Currell, B. Franzke, A. Gumberidze, J. Jacobi, P. H. Mokler, F. Nolden, U. Spillman, Z. Stachura, M. Steck, and T. Stohlker, *Phys. Rev. A* **83**, 020701(R) (2011).
- [39] Z. Hu, X. Han, Y. Li, D. Kato, X. Tong, and N. Nakamura, *Phys. Rev. Lett.* **108**, 073002 (2012).
- [40] Z. Hu, Y. Li, X. Han, D. Kato, X. Tong, H. Watanabe, and N. Nakamura, *Phys. Rev. A* **90**, 062702 (2014).
- [41] H. Jörg, Z. Hu, H. Bekker, M. A. Bleszenohl, D. Hollain, S. Fritzsche, A. Surzhykov, J. R. Crespo López-Urrutia, and S. Tashenov, *Phys. Rev. A* **91**, 042705 (2015).
- [42] K. N. Lyashchenko and O. Y. Andreev, *Phys. Rev. A* **91**, 012511 (2015).
- [43] C. Shah, H. Jörg, S. Bernitt, S. Dobrodey, R. Steinbrügge, C. Beilmann, P. Amaro, Z. Hu, S. Weber, S. Fritzsche, A. Surzhykov, J. R. CrespoLopez-Urrutia, and S. Tashenov, *Phys. Rev. A* **92**, 042702 (2015).
- [44] N. Nakamura, *J. Phys. B* **49**, 212001 (2016).
- [45] P. Amaro, C. Shah, R. Steinbrügge, C. Beilmann, S. Bernitt, Jose R. Crespo López-Urrutia, and S. Tashenov, *Phys. Rev. A* **95**, 022712 (2017).
- [46] S. N. Nahar, M. Montenegro, W. Eissner, and A. K. Pradhan, *Phys. Rev. A* **82**, 065401 (2010).
- [47] A. M. Sossah, H.-L. Zhou, and S. T. Manson, *Phys. Rev. A* **86**, 023403 (2012).
- [48] G. Breit, *Phys. Rev.* **34**, 553 (1929).
- [49] G. Breit, *Phys. Rev.* **36**, 383 (1930).
- [50] F. A. Parpia, C. F. Fischer, and I. P. Grant, *Comput. Phys. Commun.* **94**, 249 (1996).
- [51] I. P. Grant, *Relativistic Quantum Theory of Atoms and Molecules: Theory and Computation* (Springer, New York, 2007).
- [52] J. P. Desclaux, *Comput. Phys. Commun.* **9**, 31 (1975).
- [53] J. Jiang, C. Z. Dong, L. Y. Xie, J. G. Wang, J. Yan, and S. Fritzsche, *Chin. Phys. Lett.* **24**, 691 (2007).
- [54] J. Jiang, C.-Z. Dong, L.-Y. Xie, and J.-G. Wang, *Phys. Rev. A* **78**, 022709 (2008).
- [55] H. L. Zhang, D. H. Sampson, and R. E. H. Clark, *Phys. Rev. A* **41**, 198 (1990).
- [56] K. Blum, *Density Matrix Theory and Applications*, 3rd ed. (Springer-Verlag, Berlin, 2012).
- [57] E. G. Berezko and N. M. Kabachnik, *J. Phys. B* **10**, 2467 (1977).
- [58] E. G. Berezko, N. M. Kabachnik, and V. S. Rostovsky, *J. Phys. B* **11**, 1749 (1978).
- [59] V. V. Balashov, A. N. Grum-Grzhimailo, and N. M. Kabachnik, *Polarization and Correlation Phenomena in Atomic Collisions* (Kluwer Academic, New York, 2000).
- [60] S. Fritzsche, *Comput. Phys. Commun.* **240**, 1 (2019).
- [61] U. I. Safronova and A. S. Shlyaptseva, *Phys. Scr.* **54**, 254 (1996).
- [62] V. A. Yerokhin, A. Surzhykov, and S. Fritzsche, *Phys. Rev. A* **90**, 022509 (2014).
- [63] Z. W. Wu, M. M. Zhao, C. Ren, C. Z. Dong, and J. Jiang, *Phys. Rev. A* **101**, 022701 (2020).
- [64] Z. W. Wu, J. Jiang, and C. Z. Dong, *Phys. Rev. A* **84**, 032713 (2011).
- [65] See Supplemental Material at <http://link.aps.org/supplemental/10.1103/PhysRevA.105.032809> for the data used to plot this and the following figures.